

PLASMA TEMPERATURE AND ABUNDANCE DISTRIBUTIONS OF RICH CLUSTERS OF GALAXIES

K. Yamashita, M. Watanabe, A. Furuzawa, and Y. Tawara

Department of Physics, Nagoya University
Furo-cho, Chikusa-ku, Nagoya 464-8602, Japan

We have carried out the spectro-imaging analysis of rich clusters of galaxies, such as the Coma cluster, the Ophiuchus cluster and A2319 observed by ASCA. Mean temperatures of these clusters were obtained to be 9-11 keV. X-ray images in the energy bands, 0.7-3 keV, 3-10 keV and 0.7 keV were derived by iteratively deconvolving observed data with the response function of X-ray telescope and the plasma temperature. Thus the surface brightness distribution and temperature map for these three clusters were obtained with the angular resolution of 2 arcmin and 8 arcmin, respectively. It turned out that the high temperature regions (>12 keV) are largely extended in the outer envelope and the low temperature regions (<8 keV) correspond to the image excess. These results could be interpreted by cluster-cluster and subcluster-cluster merging process. The Ophiuchus cluster significantly shows the abundance anisotropy, that is, low in the central region and high in the outer envelope.

1 Introduction

Rich clusters of galaxies have been considered as a dynamically well-relaxed system confined in a gravitational potential and show isothermal, spherically symmetric structure. Recent X-ray spectro-imaging and imaging-spectroscopic observations make clear the detailed surface brightness and temperature distributions of intracluster medium (ICM). These facts make it possible to further investigate the dynamical evolution of clusters of galaxies incorporated with optical observations of member galaxies, such as galaxy type, density distribution, radial velocity, color, magnitude and so on. Simulations of cluster merging are extensively studied and well describe the time dependent feature of surface brightness and temperature taking into account the mass ratio, velocity, separation, temperature and viewing direction from merging axis (Roettiger, et al. 1997; Takizawa 1999). We present the observational results of three nearby rich clusters of galaxies, such as the Coma cluster, the Ophiuchus cluster and A2319 observed with ASCA.

The X-ray images of the Coma cluster were observed by Einstein (Jones & Forman 1999), EXOSAT (Branduardi-Raymont et al. 1985), ROSAT (Briel et al. 1992; White et al. 1993; Vikhlinin et al. 1994, 1997) and ASCA (Honda et al. 1996; Watanabe et al. 1999). The substructure of X-ray images were extensively investigated in comparison with optical observations (Mellier et al. 1988; Colless & Dunn 1996; Biviano et al. 1996). The mean temperature over the whole cluster was obtained to be 8.5 keV by Tenma (Okumura et al. 1988), EXOSAT (Hughes et al. 1988a, 1988b) and Ginga (Hatsukade 1989). ASCA observations (Honda et al. 1996) revealed the large-scale inhomogeneity of temperature in the range of 5-11 keV. Furthermore Watanabe et al. (1999) derived the temperature map with angular resolution of 8 arcmin.

The Ophiuchus cluster is a nearby rich cluster located in the direction near the galactic center ($l=0.5$, $b=9.4$), which was identified in the crowded area by optical observations (Johnston et al. 1981; Wakamatsu & Malkan 1981). The X-ray images were observed by Einstein HRI (Arnaud et al. 1987) and ASCA (Matsuzawa et al. 1996). X-ray spectra over the whole cluster were obtained by HEAO-1 A2 (Johnston et al. 1981), Einstein, EXOSAT (Arnaud et al. 1987), Tenma (Okumura et al. 1988) and Ginga (Kafuku et al. 1992). These results show the temperature in the range of 9-11keV, the iron abundance of 0.16-0.49 relative to the cosmic. Tenma observation clearly distinguished iron K_{α} and K_{β} emission lines with gas scintillation proportional counters. Matsuzawa et al. (1996) examined the radial distribution of temperature

Table 1: Observation log and X-ray properties of three clusters

Cluster	Redshift	No. of pointings	Obs. Time	Total counts	Temp. (keV)	Abund. to solar	Core radius	β
Coma	0.0235	14	116ks	550k	9.2	0.27	9.3'	0.66
Oph	0.028	5	40ks	120k	10.9	0.34	4.9'	0.77
A2319	0.0529	2	34ks	185k	10.5	0.28	7.3'	0.27

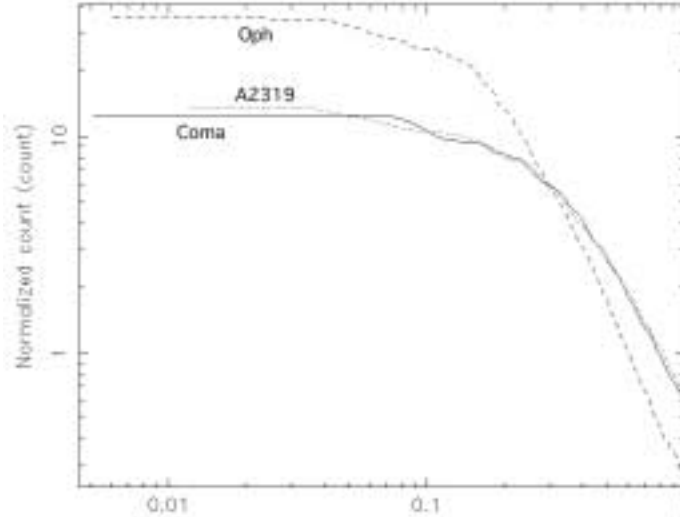


Figure 1: Radial profiles of three clusters. Solid line: Coma, dashed line: Ophiuchus and dotted line: A2319

and metal abundance in the central region within the radius of 13.8' using ASCA data. They could not find any significant variations, whereas Watanabe (2000) revealed inhomogeneous distribution of temperature and abundance within the radius of 30'.

The X-ray image of A2319 was observed by ROSAT (Feretti et al. 1997) and ASCA (Watanabe 2000), which is similar to the Coma cluster. The temperature was obtained to be 9-10 keV by Einstein MPC (David et al. 1993) and Ginga. Oegerle et al. (1995) studied the dynamical structure by optical observation, showing two clusters in projection.

2 Observations and analysis method

These clusters were observed by number of different pointings with ASCA to cover the angular extent of a whole cluster. Complete X-ray images were taken with two GIS detectors (GIS2 and GIS3), whereas SIS detectors partially covered the region due to smaller FOV (22x22). These data were screened with ASCA standard processing tools (Arnaud 1993) based on the criteria of minimum earth elevation angle of 5 deg and a cut off rigidity of 6 GeV/c. Observed GIS images are combined together after correction of exposure time, boresight and subtraction of background. The observation log of three clusters are shown in Table 1 together with X-ray properties. Temperature and abundance were derived by spectral fitting in the central region within the radius of 10 arcmin. The radial profiles of surface brightness distributions are shown in Fig. 1 in the absolute distance scale with $H_0=50$ km/sec/Mpc.

2.1 Spectro-imaging analysis

After the subtraction of the standard background used for the cluster analysis we construct X-ray images in three energy bands divided into 0.5-10 keV (total band), 0.5-3.0 keV (soft band) and 3.0-10.0 keV (hard band) over the whole cluster. The total band image is binned into a pixel of 2'x2'. A pixel size of the soft and hard band images is made larger to be 8'x8' for deriving the Hardness Ratio (HR) with good statistics. We exclude pixels whose number of counts are less than 20 for the total band and 200 for the soft and hard band from the image analysis because of their large statistical uncertainty.

ASCA X-ray telescope (XRT) has a complex point spread function (PSF) which depends on incident energies and off-axis angle from the optical axis of XRT. Our analysis took into account this effect as described in Watanabe et al. (1999) in detail. The observed image is deconvolved with the response function to produce the initial one.

We start simulating X-ray images of clusters in the soft, hard and total bands with the initial conditions of an isothermal temperature of 8-10keV depending on individual cluster and a spherically symmetric image with the β -model. We estimate the difference of images and HRs between the data and the simulated values and adjust the source image and temperature distribution. Again, we perform the second simulation with corrected image and temperature distribution. The deconvolution process is carried out in such a way of iterating this simulation until the difference between data and simulated values is smaller than systematic and statistical errors. HR is converted to a plasma temperature (kT) on the assumption of a single temperature. kT-HR relation is estimated from the ASCA full simulation as a function of off-axis angle.

2.2 Spectral fitting

In order to confirm the temperature distribution derived by HR mentioned above, we perform the spectral fitting of Raymond-Smith model to observed spectra of GIS and SIS in subdivided regions by referring to the temperature map. We derived plasma temperatures and iron abundance relative to the solar value, e.g., $N(\text{Fe})/N(\text{H})=4.68 \times 10^{-5}$ (Anders and Grevesse 1989). The hydrogen column density was fixed at the galactic value in each direction. We also fit the spectra with a thermal bremsstrahlung of single temperature and Gaussian lines to derive the ionization temperature and line energies and intensities of Fe- K_{α} . SIS detectors make it possible to resolve He-like and H-like Fe- K_{α} lines. The ionization temperatures were separately obtained by the intensity ratio of He-like and H-like Fe- K_{α} lines and compared with the electron temperature derived from the continuum component. The selection of the energy region is important for the spectral analysis. We used the galactic ridge background in the 0.7-10 keV region and ASCA standard background in the 3-10 keV region for the Ophiuchus cluster, since it lies in the direction near the Galactic center.

3 Surface brightness and temperature distribution

The temperature map (color code) and surface brightness (contour) distribution in the total band thus obtained for each cluster are shown in Fig. 2, 3, and 4. Typical errors for temperatures are estimated to be 1.5 keV in the central region and 2-6keV in the outer region, which are caused by statistics and the sensitivity of HR to temperatures. The radial profile of the surface brightness distribution is well fitted by β model as shown in Fig. 1. Core radii and β values for each cluster are summarized in table 1. The image excess from β model is also shown in Fig. 2, 3 and 4 together with the surface brightness distribution.

In general hot regions (kT>12 keV) spreads out to the outer envelope, while cool regions correspond to the image excess.

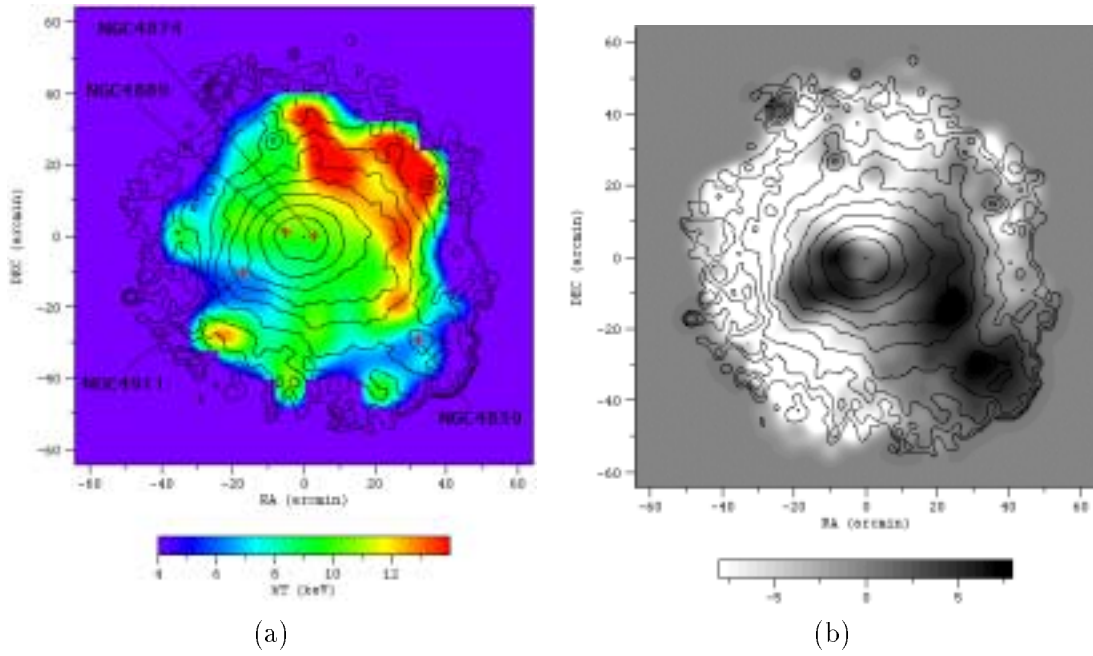


Figure 2: Temperature map shown by color code (a) and image excess by gray scale (b) for the Coma cluster superposed on the contour map of the total band. The image center: R.A.=194.9278 deg, Dec.=27.9707 deg (J2000).

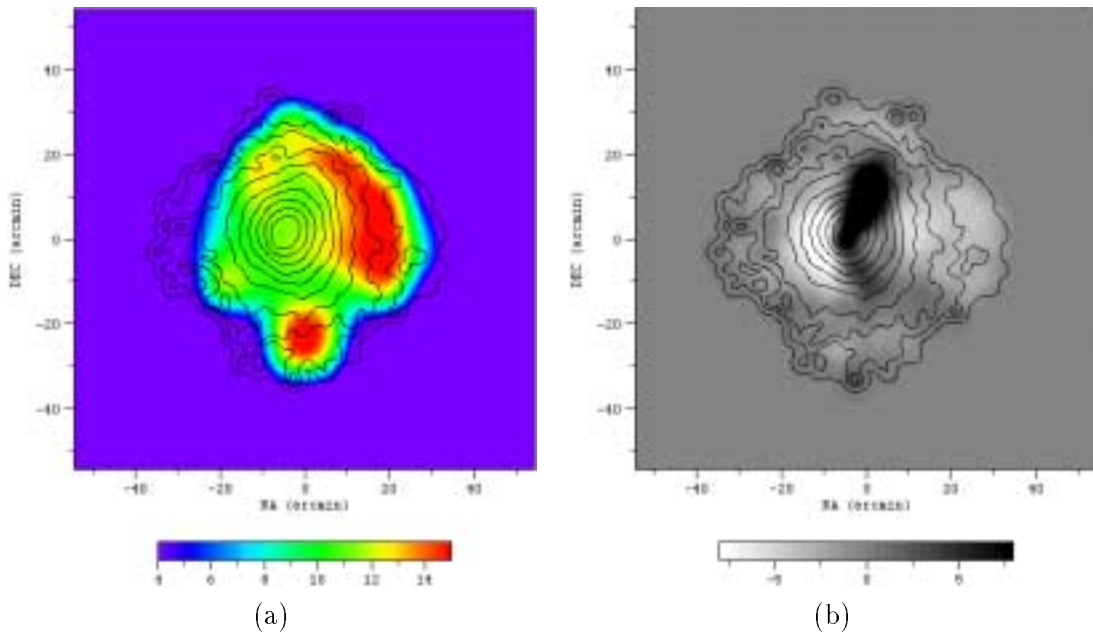


Figure 3: Same as Fig. 2 for the Ophiuchus cluster. The image center: R.A.=258.0192 deg, Dec.=-23.386 deg (J2000).

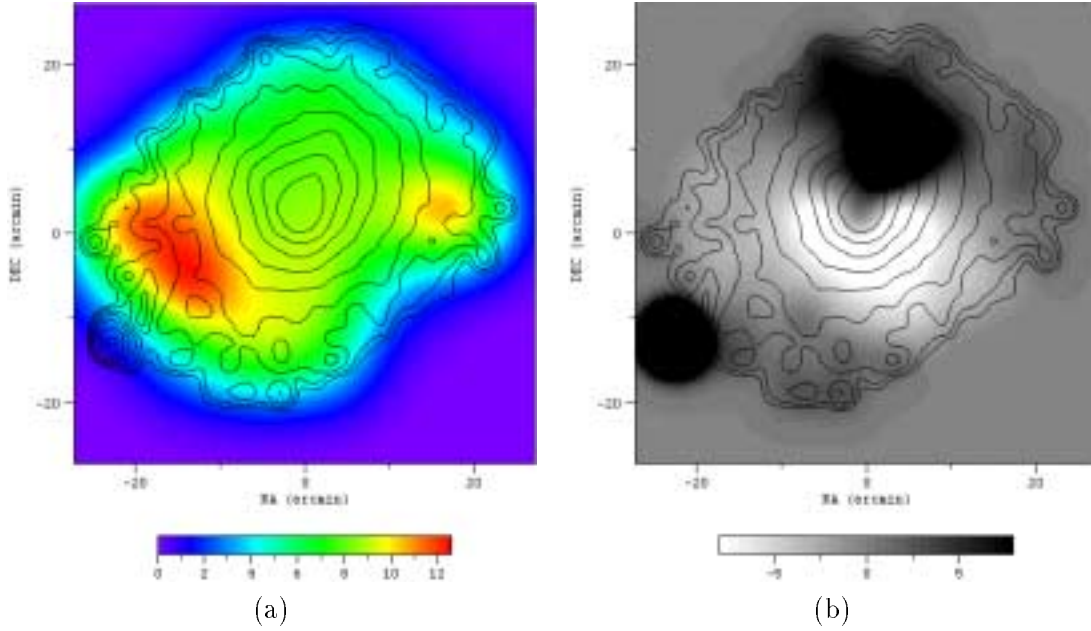


Figure 4: Same as Fig. 2 for A2319. The image center: R.A.=290.139 deg, Dec.=44.012 deg (J2000).

4 Plasma temperature and abundance

The best fit parameters of GIS spectra are summarized in Table 1, which were derived by the spectral fitting of observed data in 0.7-10keV to Raymond-Smith model in the central region within the radius of 10 arcmin. The plasma temperatures in subdivided regions are confirmed to be consistent with the temperature map. We can not see any significant difference of abundance distribution for the Coma cluster and A2319. However it was found out for the Ophiuchus cluster that the hot region in the outer envelope obviously shows higher temperature (19 keV) and higher abundance (0.82 relative to the solar value), whereas the central region shows lower temperature (10-11keV) and lower abundance (0.33).

5 Discussion

The temperature maps of three clusters derived from hardness ratio clearly show the existence of hot extended region in the outer envelope. This evidence was also confirmed by spectral fitting from which plasma temperatures were derived in several subdivided regions. Patchy temperature distribution obviously indicates that these clusters have not been dynamically well relaxed. And large-scale hot region extending more than 1Mpc could be produced by cluster merging. Simulations of the cluster merging were carried out by Roettiger et al. (1997) and Takizawa (1999). They show surface brightness and temperature distributions with elapsing time after merging. Then, we conclude this cluster would be formed by cluster merging within 1 Gyr.

The image excess shown in Fig.2, 3 and 4 coincides to the lowest temperature region. This indicates that a small group of galaxies having lower temperature is projected on or associated with the cluster. The iron abundance was obtained to be 0.33-0.89 in 6 subdivided regions for the Ophiuchus cluster. The Coma cluster and A2319 would not show significant variation of iron abundance over the whole cluster, which is 0.27 in the central region (Watanabe et al. 1997). Okumura et al. (1988) derived the iron abundance of the Ophiuchus and Coma cluster to be 0.42 and 0.27 averaged over the whole cluster by the Tenma observations respectively. This fact indicates that the Ophiuchus cluster is chemically more evolved than the Coma cluster. Allen

and Fabian (1998) examined the abundance of cooling and non-cooling flow clusters, which are 0.344 ± 0.057 and 0.207 ± 0.054 in average, respectively. The Ophiuchus cluster is more centrally concentrated and has the core radius of $4.9'$ (240kpc), while the Coma cluster has that of $9.3'$ (380kpc).

We speculate that the Ophiuchus cluster has been formed by the merging of two clusters with different abundance. The intracluster gas has not yet mixed up well, but heated up by shock wave. The abundance distribution is a good indicator for the mixing of intracluster gas caused by the merging process. It seems that the relaxation time of ICM mixing is longer than that of shock propagation. Then, relatively high temperature of these two clusters is well explained by the cluster merging.

6 Summary

We have found the observational evidence of the dynamical structure for three nearby rich clusters from the X-ray surface brightness distribution, temperature map and spectra in subdivided regions obtained by ASCA as follows.

- 1) The surface brightness distribution is nearly spherically symmetric and represented by a β -model.
 - 2) Largely-extended hot regions exist in the outer envelope with the angular size of a few 10 arcmin.
 - 3) The image excess from a spherically symmetric β -model coincides to the lowest temperature region.
 - 4) For the Ophiuchus cluster iron abundance in hot regions is higher than other regions by a factor of 2 in average, whereas other two clusters would not show any significant variation.
- These facts could be explained by the cluster merging scenario.

Acknowledgments

We thank the XRT, ASCA_ANL and SimASCA teams for building the analysis system for extended source. This work was supported in part by a Grant-in-Aid for Specially Promoted Research, contract No. 07102007, from the Ministry of Education, Science, Sports and Culture, Japan.

References

- Allen, S.W. & Fabian, A.C., *MNRAS* **297**, L63 (1998).
- Anders, E. & Grevesse, N., *Geochim. Cosmochim. Acta* **53**, 197 (1989).
- Arnaud, K.A., Johnston, R.M., Fabian, A.C., Crawford, C.S., Nulsen, P.E.J., Shafer, R.A. & Mushotzky, R.F., *MNRAS* **227**, 241 (1987).
- Arnaud, K., *ASCA Newsletter, No. 1*, (NASA/GSFC)(1993).
- Biviano, A., Durret, F., Gerbal, D., Le Fevre, O., Lobo, C., Mazure, A., & Slezak, E., *A&A* **311**, 95 (1996).
- Branduardi-Raymont, G., Mason, K.O., Murdin, P.G., & Martin, C., *MNRAS* **216**, 1043 (1985).
- Briel, U.G., Henry, J.P., & Boehringer, *A&A* **259**, L31 (1992).
- David, L., Slyz, A., Jones, C., Forman, W. & Vrtilek, S., *ApJ* **412**, 479 (1993).

- Feretti, L., Giovannini, G. & Bohringer, H., *New astronomy* **2**, 501 (1997).
- Hatsukade, I., Ph. D. Thesis, Osaka University (1989).
- Honda, H., *et al.*, *ApJ* **473**, L71 (1996).
- Hughes, J.P., Yamashita, K., Okumura, Y., Tsunemi, H., & Matsuoka, M., *ApJ* **327**, 615 (1988a).
- Hughes, J.P., Gorestein, P., & Fabricant, D., *ApJ* **329**, 82 (1988b).
- Jones, C., & Forman, W., *ApJ* **511**, 65 (1999).
- Johnston, M.D., Bradt, H.V., Doxsey, R.E., Margon, B., Marshall, F.E. & Schwartz, D.A., *ApJ* **245**, 799 (1981).
- Kafuku, S., Yamauchi, M., Hattori, H., Kawai, N. & Matsuoka, M., in *Frontiers of X-ray Astronomy*, ed Y. Tanaka, K. Koyama (Universal Academy Press, Tokyo), P483 (1992).
- Matzuzawa, H., Matsuoka, M., Ikebe, Y., Mihara, T., & Yamashita, K., *PASJ* **48**, 567 (1996).
- Oegerle, W., Hill, J. & Fitchett, M., *AJ* **110**, 32 (1995).
- Okumura, Y., Tsunemi, H., Yamashita, K., Matsuoka, M., Koyama, K., Hayakawa, S., Masai, K. & Hughes, J.P., *PASJ* **40**, 639 (1988).
- Roettiger, K., Loken, C. & Burns, J., *ApJS* **109**, 307 (1997).
- Takizawa, M., *ApJ* **520**, 514 (1999).
- Wakamatsu, K. & Malkan, M.A., *PASJ* **33**, 57 (1981).
- Watanabe, M. Yamashita, K., Furuzawa, A., Kunieda, H., Tawara, Y. and Honda, H., *ApJ* **527**, 80 (1999).
- Watanabe, M., Ph. D Thesis, Nagoya University (2000).